

Tech Memo
AP 23

AD-A269 561



Technical Memorandum
February 1993

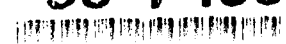
Comparison between Swept and Delta Canards on a
Model of a Combat Aircraft

by

D. G. Mabey
C. R. Pyne

Bedford, Bedfordshire

93-21953



This Memorandum has been prepared for MOD and, except as indicated, may be used and circulated in accordance with the arrangements of:

Technical memorandum AP 23

It may not, however, be used or copied for any non-Government or commercial purposes without the written agreement of DRA

Requests for reproduction should be made to:

DRA Intellectual Property Department

Tel: (0252) 392626

CONDITIONS OF RELEASE

0148887

318039

DRIC U

CROWN COPYRIGHT (c)
1992
CONTROLLER
HMSO LONDON

DRIC Y

Reports quoted are not necessarily available to members of the public or to commercial organisations.

DEFENCE RESEARCH AGENCY

Bedford

Technical Memorandum Aerodynamics/Propulsion 23

Received for printing 11 February 1993

COMPARISON BETWEEN SWEEPED AND DELTA CANARDS ON A MODEL OF A COMBAT AIRCRAFT

by

D. G. Mabey

C. R. Pyne

SUMMARY

The aerodynamic characteristics of a low speed half model of a typical combat aircraft configuration fitted with a 65° delta canard planform are compared with those for the same model fitted with 44.3° swept canard. Both canards had an RAE 104 aerofoil section. The tests were made in the DRA 13 ft \times 9 ft Wind Tunnel on a large model of the DRA High Incidence Research Model (HIRM 1), modified to represent the Experimental Aircraft (EAP) configuration.

For a 15% smaller planform area, the delta canard gives higher lift and comparable pitching moments for trimming. For canard and wing buffeting the differences are small.

Overall, these low speed measurements suggest that delta canards with round leading edges have significant advantages over swept canards for future combat aircraft.

This research was conducted for the Ministry of Defence under package 7B item FO7B98XX.

© Crown Copyright (1993)
Defence Research Agency
Farnborough Hampshire GU14 6TD UK

DTIC QUALITY ASSURANCE

Accession For		
NTIS	CRA&I	<input checked="" type="checkbox"/>
DTIC	FAB	<input type="checkbox"/>
Unannounced		<input type="checkbox"/>
Justification		
By		
Distribution/		
Availability Codes		
Dist	Avail. and/or Special	
A-1		

LIST OF CONTENTS

		Page
1	INTRODUCTION	3
2	EXPERIMENTAL DETAILS	4
	2.1 Canards	4
	2.2 Analysis of measurements	4
	2.3 Test conditions	5
3	RESULTS	6
	3.1 Overall static forces and moments	6
	3.2 Wing and canard buffeting	7
	3.2.1 Wing buffeting	7
	3.2.2 Canard buffeting and canard static bending moments	8
	3.3 Interaction between the canard and wing flows in the (α, η_c) domain	10
4	CONCLUSIONS	11
	Table 1	13
	List of symbols	14
	References	15
	Illustrations	Figures 1-12
	Report documentation page	inside back cover

1 INTRODUCTION

A detailed study of the steady and time-dependent aerodynamic characteristics at low speeds on advanced combat aircraft configurations fitted with canards is being made with a large half model of the RAE High Incidence Research Model (HIRM 1) in the DRA 13 ft x 9 ft Wind Tunnel. This study has the prime objective of optimising both the canard and wing design at cruise conditions, without prejudicing the aircraft performance when manoeuvring at high lift coefficients. The model can be modified to represent the Experimental Aircraft Project (EAP) configuration with an undrooped leading edge (Fig 1). During a previous investigation¹ this wing configuration was used to show that a delta canard (of the same area) could replace the swept canard currently used, giving an increase in control power of approximately 15% without any adverse effects on the wing buffeting. However, a delta canard is less compact, and when deflected it has larger gaps than the swept canard. Despite these disadvantages the delta canard should give lower wave drag at supersonic speeds, due to the effects of increased sweep and possibly due to an improved area distribution. In addition the greater sweep of the delta canard should reduce the aircraft radar signature.

In the previous investigation¹ the improved control power was achieved even through the delta canard (selected because buffeting measurements were available²) had an unrealistic section; a flat plate of constant thickness with a bevelled leading edge and a bluff trailing edge (Fig 2a). This section inevitably gave a large drag penalty. Accordingly Ref 1 recommended that a further test should be made on a delta planform with a realistic, RAE 104 section which would have no base drag. For this new canard the area was reduced by 15% (Fig 2b) in an attempt to generate the same control power as the swept canard (Fig 3) and to provide a further reduction in drag. This Memorandum reports steady and unsteady measurements with swept and smaller delta canard, and confirms the advantages of the smaller delta canard for a combat aircraft.

In the previous tests the local pressures induced at three sections on the wing (shown in Fig 1) by sinusoidal oscillation of both the delta canard and the swept canard were found to be small and comparable¹. Hence in the present tests no oscillatory pressures were measured.

Previous research³⁻⁵, on the various configurations of the HIRM 1 model showed how the canard effective incidence controls the canard/wing interaction. This was illustrated again for the present tests during the analysis of the steady measurements. For brevity the time-dependent measurements have not been analysed in detail.

2 EXPERIMENTAL DETAILS

Complete descriptions of the model are included in Refs 3 and 5 and are summarised here. The model is mounted on the half model balance in the floor of the DRA 13 ft x 9 ft Wind Tunnel so that the overall steady forces can be measured.

The wing motion in the first bending mode at $f = 22$ Hz is measured by an accelerometer near to the tip (at $\eta = 0.8$). All the unsteady signals were recorded using an updated version of the DRA Presto system⁶.

2.1 Canards

Fig 2a shows the larger, 65° delta canard used in the test of Ref 1, which has the same area as the swept canard (Fig 3). Fig 2b shows the new, smaller 65° delta canard, which has an area 85% of that of the swept canard and an RAE 104 section. It is important to notice that due to the reduced root chord of the smaller delta canard, the gap between the canard and the fuselage (due to fuselage curvature) is much smaller, particularly for the larger, negative canard settings ($\eta_c = -25^\circ$ and -41°).

Both canards are of similar construction and have a pair of glass fibre skins which are stiffened internally with polyurethane foam. The canard loads are diffused from this relatively weak structure into a steel root block, which has a strain gauge bridge configured to measure the bending response in the usual way⁷. The tip of the small delta canard was cropped slightly and made of aluminium for ease of manufacture. The first bending frequencies of the swept and delta canards were 58 and 140 Hz respectively. For the delta canard some measurements were given for a second mode at 345 Hz.

2.2 Analysis of measurements

For the small delta canard the canard-root bending moment coefficient is given by

$$C_{BC} = \frac{\text{canard bending moment}}{qS_c(0.333s_c)} \quad (1)$$

where $S_c =$ exposed area (0.0774 m²)

and $s_c =$ exposed canard semi-span (0.088 m).

The factor 0.333 is introduced into the denominator of equation (1) to make the measured bending moment equivalent to a lift coefficient appropriate to a lift force acting at the centre of area of the planform, which is almost triangular.

The usual frequency bandwidth selected for tests with the Presto system in the DRA 13 ft x 9 ft Wind Tunnel is 0-100 Hz and the standard measurement time is 30 s. This gives about 660 cycles of buffeting at the wing first bending frequency (22 Hz). The first

bending frequency of the small delta canard is 140 Hz, outside the usual measurement bandwidth of the computer anti-alias filters then available. Hence the unfiltered signals at 140 Hz were measured with a spectrum analyser (Brüel and Kjaer Type 2120).

Buffeting response is measured as output from the strain-gauge bridge. Ideally, for the wing the buffet excitation parameter in any mode is given by the relation^{7,8}

$$\sqrt{nG(n)} = \frac{2}{\sqrt{\pi}} \frac{m\ddot{z}}{qS_w} \zeta^{1/2} \quad (2)$$

where m = generalised mass in mode with respect to motion at tip,

\ddot{z} = rms tip acceleration in mode,

q = kinetic pressure,

S_w = exposed wing reference area

and ζ = total damping - as a ratio of critical damping.

However, here the main interest is the direct comparison of the wing buffeting with either the small delta canard or with the swept canard. For this purpose it is sufficient to consider the output from the strain gauge bridge (in mV) at 22 Hz plotted against the angle of incidence or the lift coefficient.

Equation (2) could not be applied for either of the canards (using S_c instead of S_w) because it proved impossible to obtain accurate values of the generalised mass for the bending modes*. Hence the canard root strain signals (in mV measured by the spectrum analyser) were compared with previous buffeting measurements on an isolated 65° delta wing with a similar geometry⁴.

2.3 Test conditions

A roughness band 3 mm wide of 0.30 to 0.36 mm diameter ballotini was applied to fix transition at 3 mm from the leading-edge of both the wing and the canard. The measurements presented were made at a speed of 60 m/s, giving a Reynolds number of 3.7×10^6 based on the wing aerodynamic mean chord, \bar{c} .

No corrections were made for tunnel interference. In this closed working section, corrections would be large for such a large half model, particularly at angles of incidence from 15-30° when the wing flow is well separated. The uncorrected steady lift coefficient

* An attempt was made to measure the generalised mass in the usual way by adding small masses to the tip of the canard and noting the change in frequency. However, due to the high level of structural damping, and the corresponding flatness of the spectral peaks, these small changes in frequency could not be measured accurately.

will have large errors (up to 0.1 in C_L) following flow separation. This is shown by the comparisons of uncorrected and corrected lift curves (Ref 9, Fig 26) for a combat aircraft half model of almost the same semi-span ($s_w = 1350$ mm compared to $s_w = 1300$ mm) and much the same planform (compare Fig 8 of Ref 9 with Fig 1) also tested in the DRA 13 ft \times 9 ft Wind Tunnel. However wall corrections are unlikely to affect the character of the interactions between the canard and wing flows, which is the main objective of these tests.

The static forces and moments measured by the balance and the model motion measurements were restricted generally to $\alpha = 0^\circ, 5^\circ, 10^\circ, 12^\circ$ (buffer onset), $15^\circ, 20^\circ, 25^\circ$, and 30° . The small delta canard was tested in August 1990. At that time the tests on the swept canard were repeated because the wing had been re-assembled twice since Ref 1 was reported.

3 RESULTS

The static force and buffeting measurements of the present tests conform, to the general character of those found in previous experiments^{3,5}. Hence it is convenient to consider the overall static forces and moments (section 3.1), the wing and canard buffeting (section 3.2) and the canard/wing flow interactions in terms of the canard effective incidence (section 3.3).

It is helpful to recall the main conclusions from the earlier tests with the swept canard⁵. The wing-strake vortex inhibits the growth of bubble separations on the wing, increases lift and reduces buffeting (Fig 4). The further effect of a swept canard (for positive canard effective incidence) enhances the favourable effect of the strake vortex. This beneficial effect of the canard is small compared to the large favourable effect of the strake.

3.1 Overall static forces and moments

Fig 5 shows that the effect of both the canards on the overall lift is much the same. For the small delta canard (Fig 5a) the lift increases steadily with incidence so that at $\alpha = 30^\circ$ a lift coefficient of $C_L = 1.66$ is developed for $\eta_c = -5^\circ$. The measurements for the swept canard (Fig 5b) are similar in character but generally a little lower at the higher angles of incidence, eg at $\alpha = 30^\circ$, $C_L = 1.60$ for $\eta_c = -5^\circ$. We shall see later (section 3.3) that for $\eta_c = -41^\circ$, even at $\alpha = 30^\circ$ the effective incidence, α_c , is still negative for both canards, so that the interference effect on the wing is adverse, yet small according to Ref 5. Thus Fig 5 shows that for $\eta_c = -41^\circ$ the lift curves for both delta and swept canards are virtually identical and below the 'canard off' values (equivalent to $\alpha_c = 0^\circ$ according to Refs 3 and 5) which are included only in Fig 5b.

Fig 6 shows that the effects of each canard on the pitching moment characteristics are virtually identical, ie that the control power of the small delta canard is the same as that

of the larger swept canard, as inferred from the tests of Ref 1. For $\eta_c = -41^\circ$ both canards start to lose effectiveness below $C_L = 0.6$. This is probably due to the canard stalling (as illustrated in Figs 9a and 10a). However, this is of minor importance because such an extreme negative setting is unlikely to be used at low angles of incidence.

Fig 7 illustrates the effect of the canards on the overall lift and drag characteristics. For a given canard setting the trimmed C_L values are about the same with the small delta and swept canards (Fig 7a), as are the corresponding Lift Drag (L/D) ratios when expressed as a function of trimmed C_L (Fig 7b). The improvement of the drag characteristics with the small delta canard (compared to the tests of Ref 1) is due to the combined effects of the elimination of the base drag and the smaller area. It is interesting to note that the measurements with the swept canard have repeated well, even though the wing has been reassembled twice since the original tests.

3.2 Wing and canard buffeting

3.2.1 Wing buffeting

Fig 8 shows that the addition of either canard for both $\eta_c = -10^\circ$ and -41° only makes relatively small changes to the low levels of the wing buffeting signal below $\alpha = 12^\circ$ in the first bending mode. With respect to the variation with the angle of incidence, for $\eta_c = -10^\circ$ the canard effective incidence (defined later) is always positive so that the interference on the wing is favourable. The wing buffeting is much the same for both canards and significantly lower than for the wing alone (Fig 8a). In contrast for $\eta_c = -41^\circ$ the canard effective incidence is generally negative and the interference on the wing is unfavourable. The wing buffeting is much the same for both canards and generally comparable with the wing alone (Fig 8b). For both canards at $\eta_c = -41^\circ$ the measurements were extended down to $\alpha = 0^\circ$, although this represents an unrealistic flight condition. Normally high negative canard settings would be utilized only for recovery at high angles of incidence. A high negative canard setting should never be combined with such a low incidence. When this unrealistic condition does obtain the buffet excitation from the separated flow on the lower surface of the canards excites the wing, when the wing flow is itself attached. This wing motion causes a feedback process which increases the canard buffeting, to be discussed later and shown in Fig 10b. When the wing buffeting measurements are plotted against the overall lift coefficient, the effects of the canards on the overall lift (an increase for $\eta_c = -10^\circ$ in Fig 8c and a decrease for $\eta_c = -41^\circ$ in Fig 8d) show that the improvements in lift coefficient for a given level of wing buffeting are significant for $\eta_c = -10^\circ$, but not for $\eta_c = -41^\circ$.

3.2.2 Canard buffeting and canard static bending moments

For both the delta and swept canards, buffeting signals and static bending moment coefficients, C_{BC} were measured with $\eta_c = -5^\circ, -10^\circ, -25^\circ$ and -41° over the incidence range from $0 \leq \alpha \leq 30^\circ$.

For the delta canard Fig 9a shows that for all canard settings C_{BC} increases steadily with α except for $\eta_c = -41^\circ$ when the canard is stalled on the lower surface for $\alpha \leq 5^\circ$, as in the tests with the larger canard in Ref 1. However $\eta_c = -41^\circ$ is an unrealistic setting for $\alpha \leq 5^\circ$ as already mentioned in section 3.2.1 above.

Fig 9b shows the corresponding canard buffeting signals at 140 Hz. The unusual feature of these measurements is that for $\eta_c = -41^\circ$ with the canard stalled at $\alpha = 5^\circ$ the buffeting is high (350 mV), as in the tests of Ref 1. Thereafter the buffeting decreases as α increases, reaching a minimum at $\alpha = 20^\circ$ before increasing again. This variation is explained below when discussing Fig 11.

Following previous practice with diverse canard/wing configurations^{3,5,11,12}, the canard static bending moment coefficients, C_{BC} , and the buffeting signals may be expressed as unique functions of canard effective incidence, α_c .

For the symmetric swept canard in the tests of Ref 5 and the present tests

$$\alpha_c = (1 + k_1) \alpha + \eta_c \quad , \quad (3)$$

where k_1 = upwash factor due to the wing and the fuselage. In equation (3) k_1 is a function of η_c and has the values listed in Table 1.

Fig 10 shows that α_c (defined according to equation (3) and Table 1) gives a good correlation of both the static bending moment coefficients and the buffeting signals. However the static bending moment coefficients (Fig 10a) (with two different wing configurations) in Refs 5 and 10 are appreciably larger than those measured on the present canard. Currently no explanation can be offered for this discrepancy. However it is interesting to note that the present measurements are closer to those made on a smaller canard (with a similar shape) which was tested on a small model in Refs 11 and 12. As expected, the buffeting signals (Fig 10b) have a variation with α_c similar in shape to the measurements of the buffet excitation parameter, $\sqrt{nG(n)}$, given in Ref 5.

From the previous tests it was realised that equation (3) would not apply for the small delta canard because the apex extends forward to a section where the fuselage area is changing fairly rapidly (see discussion in Ref 1, Appendix A). Accordingly the relationship observed was of the form:

$$\alpha_c = (1 + k_1) \alpha + \eta_c + \lambda \quad , \quad (4)$$

where k_1 and λ are functions of η_c also listed in Table 1. The values of k_1 are only 85% of that for the swept canard because of the smaller area of the present delta canard (according to the theory of Ref 3, Appendix C). The variable values of λ are required to ensure that for small effective angles of incidence,

$$C_{BC} = k\alpha_c \quad (5)$$

because the present delta canard has a symmetric section. Using equations (4) and (5) the measurements for the delta canard also can be presented as a function of α_c , (Fig 11).

For the static bending moment coefficients, Fig 11a shows a unique relation between C_{BC} and α_c for all the canard settings over the wide range from about $-20^\circ \leq \alpha_c \leq 32^\circ$. This relation is in good agreement with the normal force coefficient, C_N , measured at an incidence α on the isolated delta wing of Ref 2 (with the flat, chamfered section) over the canard effective incidence range from $-10^\circ < \alpha_c < 10^\circ$. The curves deviate for $\alpha_c \geq 12^\circ$, most probably due to the change of section. The measurements of Ref 2 did agree with the C_{BC} measurements on the larger delta canard (which also had a flat, chamfered section) (Fig 2a) *cf* Ref 1, Fig 10a.

The canard buffeting signals deserve careful examination. For the first bending mode at 140 Hz (Fig 11b), α_c provides a good correlation of the measurements for $\eta_c = -5^\circ, -10^\circ$ and -25° , with buffet onset at about $\alpha_c = \pm 5^\circ$. However, for $\eta_c = -41^\circ$ radically different results are obtained. Thus with the canard stalled for $\alpha_c = -30.6^\circ$ there is a huge peak in the signal, just as there was for the larger delta canard (*cf* Ref 1, Fig 10b). For this condition examination of the wing buffeting signal indicates that here the canard separations excite wing buffeting even when the wing flow is attached (because the corresponding values of the angle of incidence, α , are low). The wing motion (buffeting induced by the canard separations) induces unsteady upwash at the canard, thus enhancing the unsteadiness of the separated flow. In contrast, for $\eta_c = -41^\circ$ and $\alpha_c = 0^\circ$ the flow on the canard is fully attached whereas the wing incidence being 29.4° according to equation (4), the wing flow is well separated. The separated flow on the wing then induces unsteady upwash at the canard, and a significant canard response. As α varies the combination of these mutually opposing trends gives a minimum in the canard buffeting for this mode at about $\alpha_c = -10^\circ$ for $\eta_c = -41^\circ$. This confirms what an interesting condition $\eta_c = -41^\circ$ represents. Normally $\eta_c = -41^\circ$ would be selected to pitch down from high angles of incidence (say $\alpha = 25-30^\circ$). Although these angles correspond to low value of canard

effective incidence (only $\alpha_c = -5.5^\circ$ and 0.7° respectively) the wing separations induce significant canard buffeting.

The unidentified mode at 345 Hz (Fig 11c) may represent canard torsion or overtone bending, or some combination of these modes. For this higher frequency mode, α_c correlates of the measurements for all four canard settings. In particular, for $\eta_c = -41^\circ$ and $\alpha_c = -30.6^\circ$, the measurements correspond quite well with the mirror image of the measurements for $\eta_c = -5^\circ$ and -10° for $\alpha_c \geq 0$. Hence for this higher frequency the wing motion (with attached flow) cannot be significant and the corresponding upwash induced by the wing motion is much smaller. In contrast, for $\eta_c = -41^\circ$ and $\alpha_c = 0^\circ$ the large wing separations still induce significant unsteadiness at the canard at this higher frequency. Hence for $\eta_c = -41^\circ$ and $\alpha_c = 0^\circ$ the canard buffeting is still appreciably higher than for the other canard settings.

It is interesting to note that for this small delta canard (with an RAE 104 aerofoil section and a round leading edge) the buffeting in both modes increases progressively with α_c . This is because the canard leading-edge vortex extends progressively inboard and downstream as α_c increases (Fig 11d). Thus this characteristic differs from that of an isolated 65° delta with a sharp leading edge². This has a constant 'plateau' level of buffeting (say $\alpha = 10-15^\circ$) and then a sudden increase at about $\alpha = 20^\circ$, when sudden vortex breakdown approaches the trailing edge. This difference in character is illustrated by the dotted curve of $\sqrt{nG(n)} \vee \alpha$ shown in Fig 11b (after Ref 2).

3.3 Interaction between the canard and wing flows in the (α, η_c) domain

For every canard setting, η_c , the incidence, α , for zero canard effective incidence, α_c , is given by

$$C_{BC} \equiv 0 \quad . \quad (6)$$

This is readily measured and is important. For this incidence the lift increments, ΔC_L , (Fig 12a) and the pitching moment increments, ΔC_M , (Fig 12b) due to the canard are small (as they should be) up to an incidence of about 18° . Above $\alpha = 18^\circ$ there are small positive increments in both the lift and the pitching moment with the canard on. This fact can be attributed either to the interaction of the narrow canard wake with the large separations above the wing or to the flow curvature at the canard at these high angles of incidence. For the condition $\alpha_c = 0$ there is a small increment in the drag coefficient comparable with the estimated flat plate turbulent skin friction on the canard up to about $\alpha = 18^\circ$ (Fig 12c). The estimated drag increments due to the skin friction are

$$\text{for the small delta canard } \Delta C_D = 0.007 \quad , \quad (7)$$

and

$$\text{for the swept canard } \Delta C_D = 0.008 \quad . \quad (8)$$

The additional drag increment above $\alpha = 18^\circ$ is due to the increased induced drag due to the increase in lift.

From equations (4) and (3) respectively for the delta and swept canards, α_c may be evaluated as a function of α for each of the four canard settings. Hence contours of constant α_c can be prepared in the (α, η_c) domain. Ideally these contours may be used to represent the measured wing and canard buffeting when the levels of the buffet excitation parameter (given by equation (2)) are available^{11,12}. However the levels of the buffet excitation parameter are not available for these tests. Hence only the values of α_c for buffet onset may be cited.

For an isolated, small delta canard contours defining buffet onset (due to the formation of a small vortex close to the leading-edge on the upper and lower surfaces) correspond to about $\alpha_c = \pm 5^\circ$ (Fig 11b). For an isolated swept canard contours defining buffet onset (due to the formation of a swept bubble close to the leading edge on the upper and lower surfaces) correspond to $\alpha_c = \pm 8^\circ$ (Fig 10b).

4 CONCLUSIONS

This Memorandum suggests six main conclusions with respect to the comparison between a small delta canard with an RAE 104 aerofoil section and a swept canard used in conjunction with an EAP type wing.

- (1) For a smaller area, the delta canard has the same general effect on the wing flow as the swept canard.
- (2) The small delta canard provides comparable control power to that of the swept canard over a wide range of incidence.
- (3) For positive canard effective incidence and hence favourable interference, the small delta canard provides a higher overall lift at a given incidence.
- (4) On the small delta canard the buffeting increases progressively with the canard effective incidence because of the progressive development of the vortex, inboard and downstream from the leading edge (Fig 11d).

- (5) For realistic conditions with positive values of canard effective incidence, the wing buffeting is reduced by both the swept and delta canards (Fig 8c).
- (6) For unrealistic conditions with negative values of canard effective incidence the wing buffeting is increased by the canard in the range of lift coefficient from about $C_L = 0.5$ to 1.0 and decreased from about $C_L = 1.1$ to 1.4 (Fig 8d).

Table 1
CONSTANTS TO DEFINE CANARD EFFECTIVE INCIDENCE

η_C (deg)	Swept canard (equation (3))	Small delta canard (equation (4))		Large delta canard (equation(4))	
	k_1	k_1	$\lambda(\text{deg})$	k_1	$\lambda(\text{deg})$
-41	0.28	0.24	4.5	0.31	6.4
-25	0.33	0.28	3.0	0.34	8.9
-10	0.43	0.37	1.5	0.43	6.4
-5	0.43	0.37	1.5	0.43	6.4

LIST OF SYMBOLS

C_{BC}	static bending moment coefficient (equation (1))
C_L, C_D, C_m	lift, drag and pitching moment coefficients
C_N	normal force coefficient
\bar{c}	aerodynamic mean chord of gross wing (0.868 m)
k	constant (equation (5))
k_1	upwash factor due to wing and body (equation (3))
L/D	lift/drag ratio
m	generalised mass
$\sqrt{nG(n)}$	buffet excitation parameter (equation (2))
$q = \frac{1}{2}\rho U^2$	free stream kinetic pressure
S	gross wing area (1.031 m ²)
S_w	exposed wing area (0.78 m ²)
S_c	exposed canard area (0.092 m ²)
s_c	exposed canard semi-span
s_w	wing semi-span from centre line
\ddot{z}	rms tip acceleration in mode
U	free stream velocity
α	wing and fuselage incidence
α_c	canard effective incidence (equation (3))
ζ	total damping fraction critical (equation (2))
$\eta = y/s_w$	semi-span ratio for wing pressure plotting section
η_c	canard setting
λ	function of η_c (equation (4))
ρ	free-stream density

REFERENCES

- | No. | Author | Title, etc |
|-----|---------------------------------------|--|
| 1 | D.G. Mabey
B.L. Welsh
C.R. Pyne | <i>The steady and time-dependent aerodynamic characteristics of a combat aircraft with a delta or a swept canard.</i>
AGARD CP 465 15, (1989) |
| 2 | D.G. Mabey
G.F. Butler | <i>Measurements of buffeting on two 65° delta wings of different materials.</i>
AGARD CP 266 16, (1977) |
| 3 | D.G. Mabey
B.L. Welsh
C.R. Pyne | <i>Interaction between the canard and wing flows on a model of a typical combat aircraft.</i>
RAE Technical Report 87019 (1987) |
| 4 | B.L. Welsh
C.R. Pyne | <i>Wing pressures induced by the oscillation of a canard on the High Incidence Research Model (HIRM 1).</i>
RAE Technical Report 86039 (1986) |
| 5 | D.G. Mabey
B.L. Welsh
C.R. Pyne | <i>Interaction between the canard and wing flows on a model typical of the EAP configuration.</i>
RAE Technical Report 87062 (1987) |
| 6 | B.L. Welsh
D.M. McOwat | <i>PRESTO – a system for the measurement and analysis of time-dependent signals.</i>
RAE Technical Report 79135 (1979) |
| 7 | D.G. Mabey | <i>Some aspects of aircraft dynamic loads due to flow separation.</i>
RAE Technical Memorandum Aero 2110 (1987) and
AGARD R750 |
| 8 | J.G. Jones | <i>A survey of the dynamic analysis of buffeting and related related phenomena.</i>
RAE Technical Report 72197 (1972) |
| 9 | P.R. Ashill
R.F.A. Keating | <i>Calculation of tunnel wall interference from wall-pressure wall-pressure measurements.</i>
RAE Technical Report 85086 (1985) |
| 10 | D.G. Mabey
B.L. Welsh
C.R. Pyne | <i>Effects of boundary-layer fences on canard control power and power and buffeting.</i>
RAE Technical Memorandum Aero 2097 (1987) |
| 11 | D.G. Mabey
B.L. Welsh | <i>Wing and canard buffeting on a flutter model of the EAP aircraft.</i>
RAE Technical Report 8609 (1986) |

REFERENCES (concluded)

No.	Author	Title, etc
12	D.G. Mabey B.L. Welsh	<i>Further measurements of wing and canard buffeting on a flutter model of the EAP aircraft and some flight comparisons.</i> RAE Technical Report 87017 (1987)

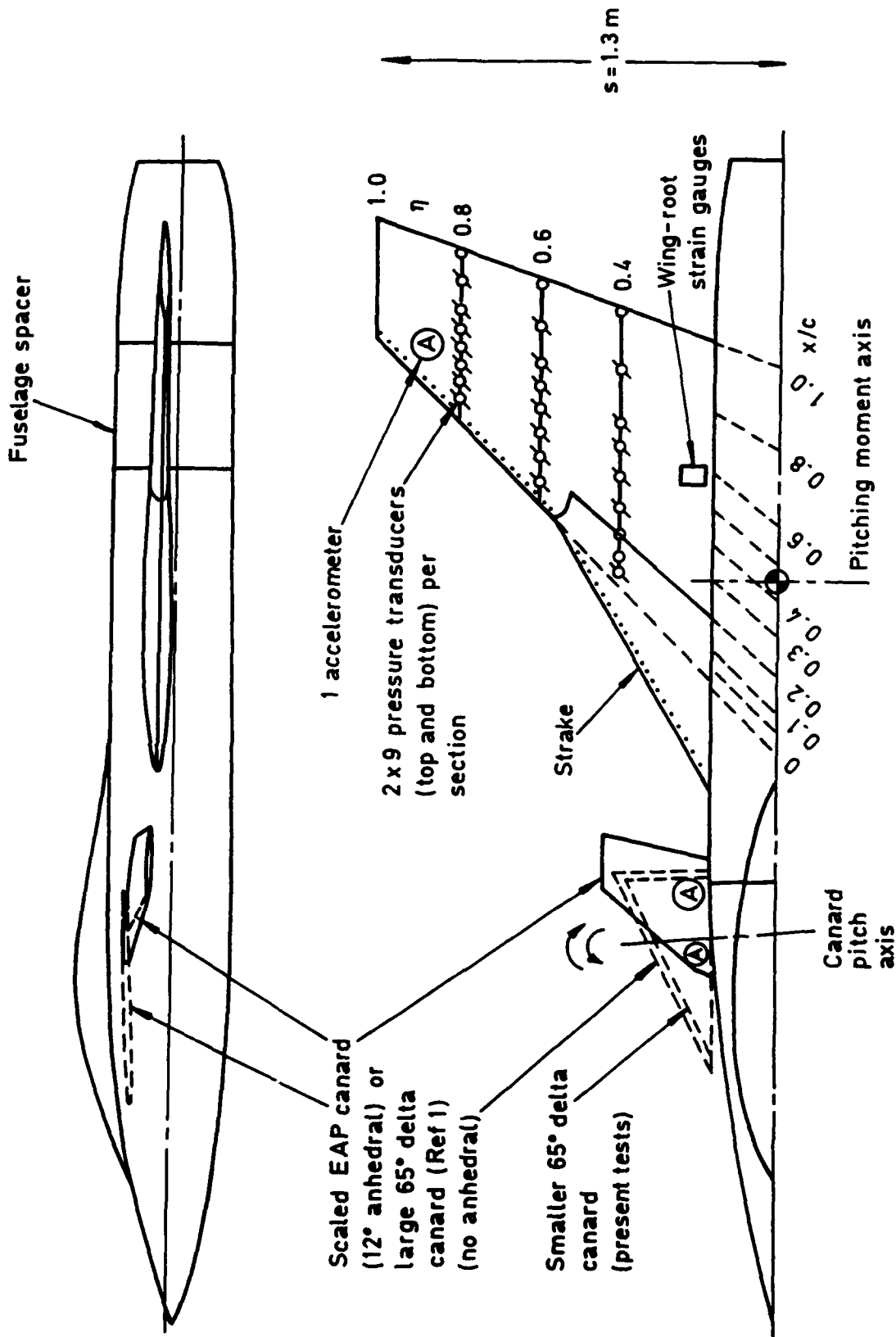
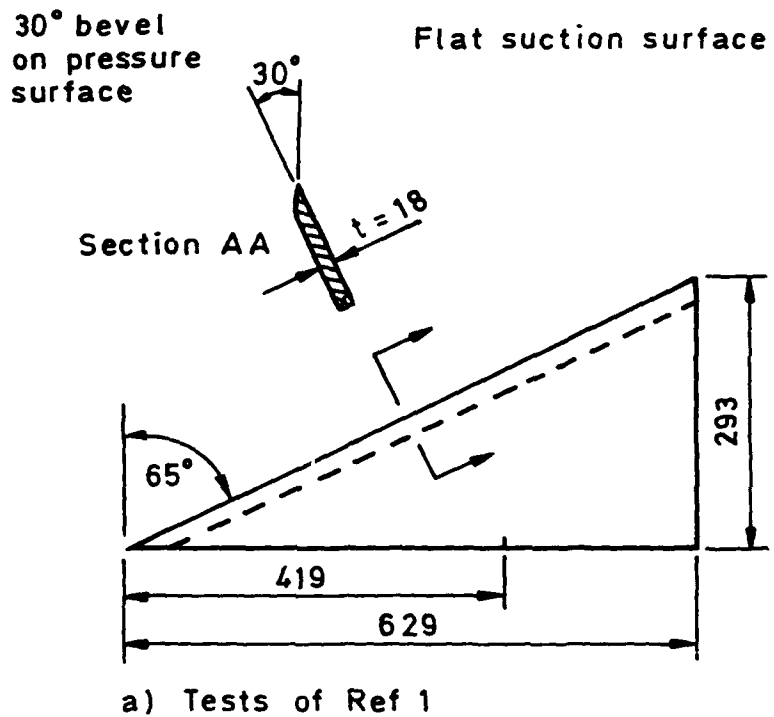


Fig 1

Fig 1 Details of model

Fig 2



Dimensions in mm

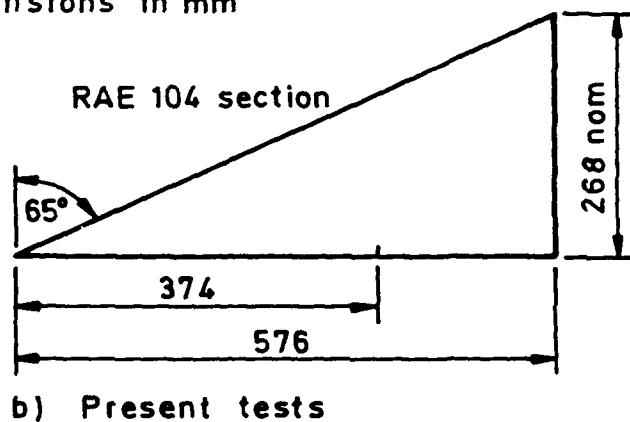


Fig 2 Details of 65° delta canards

Fig 3

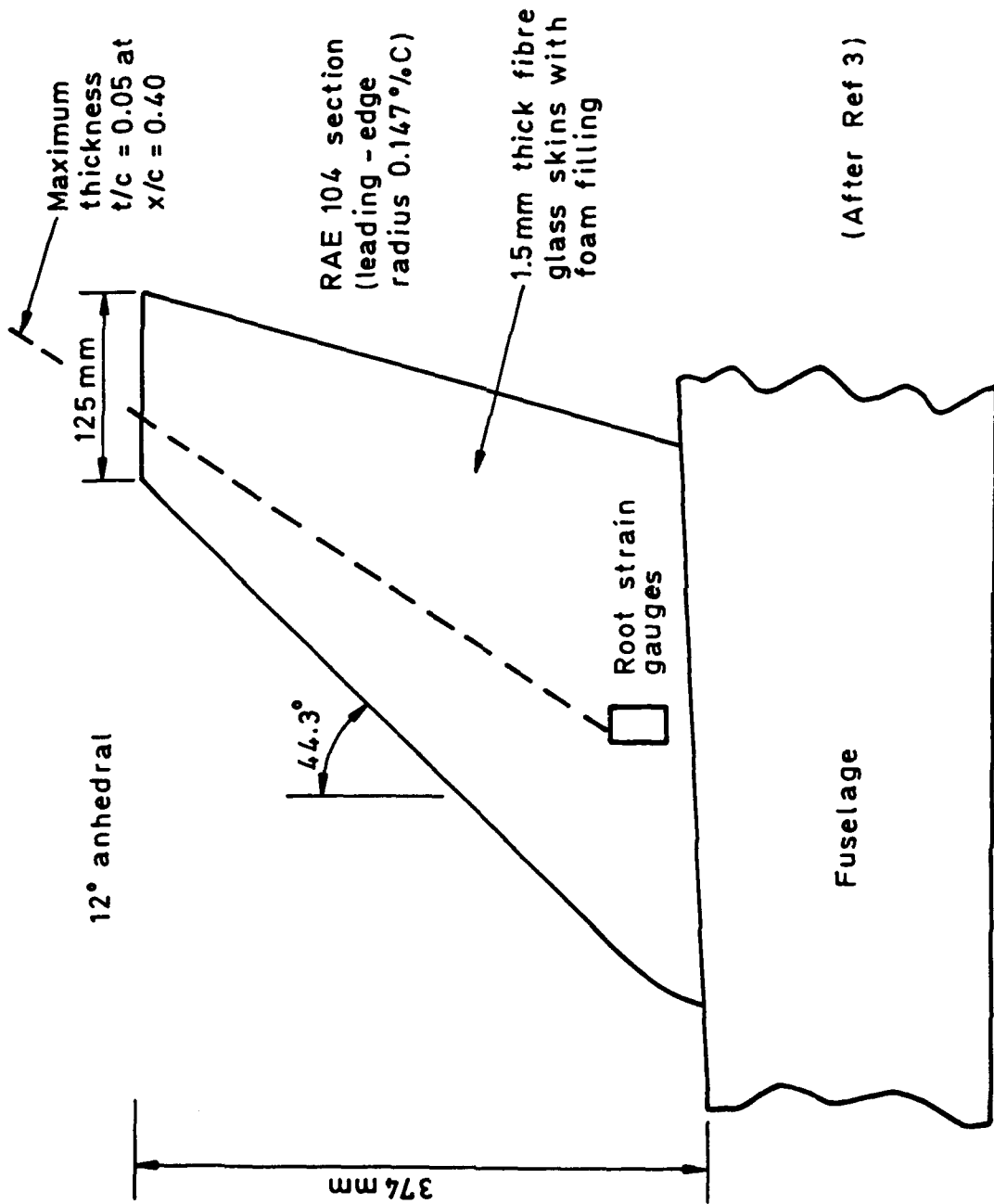


Fig 3 Details of swept canard

Fig 4

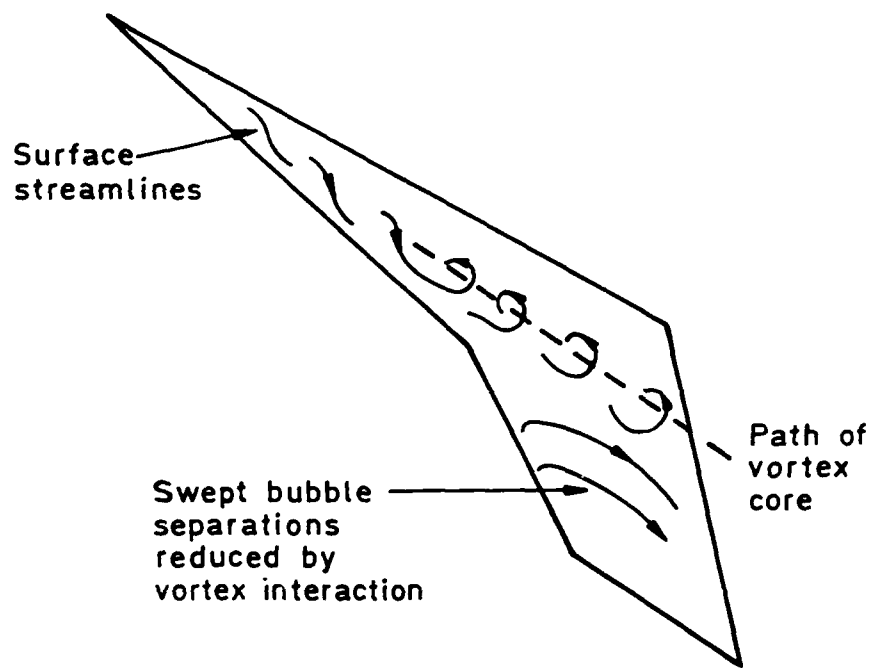


Fig 4 Effect of strake vortex on wing flow

Fig 5

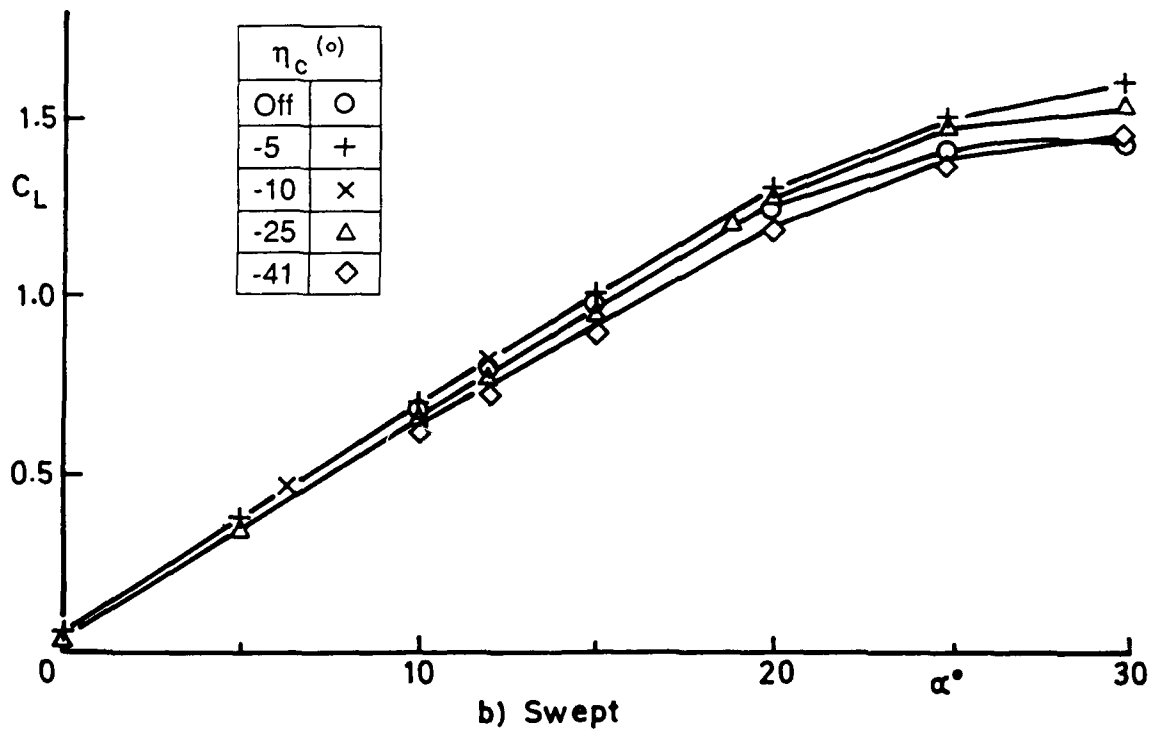
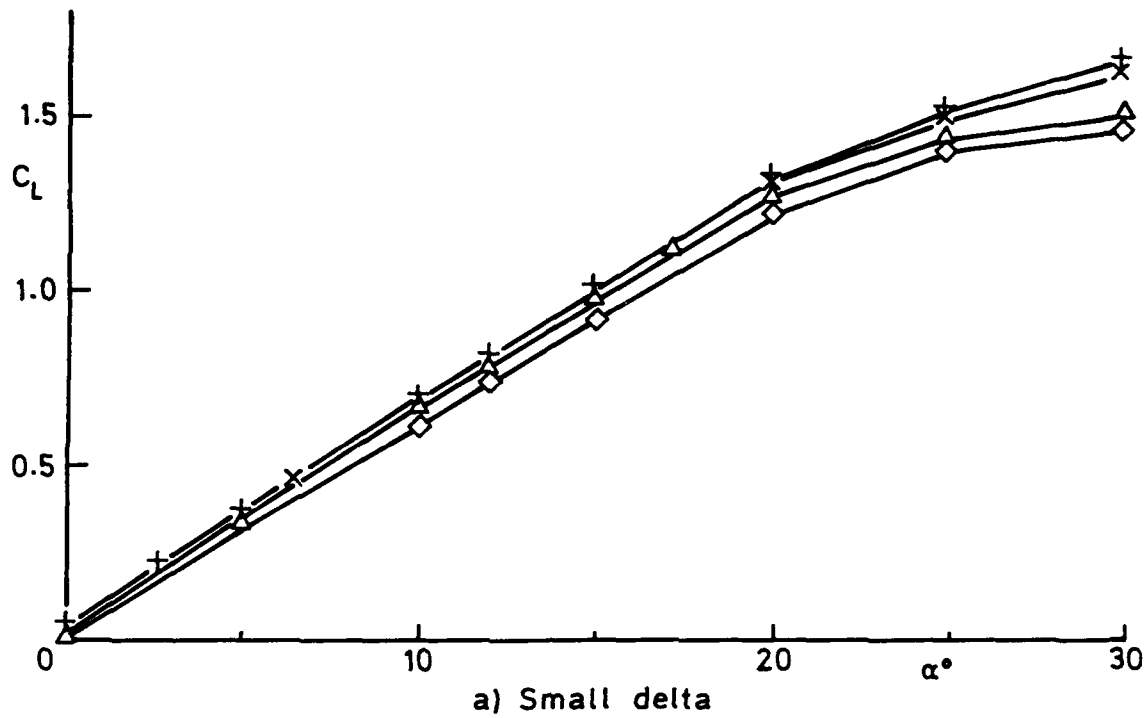


Fig 5 Effect of canards on lift

Fig 6

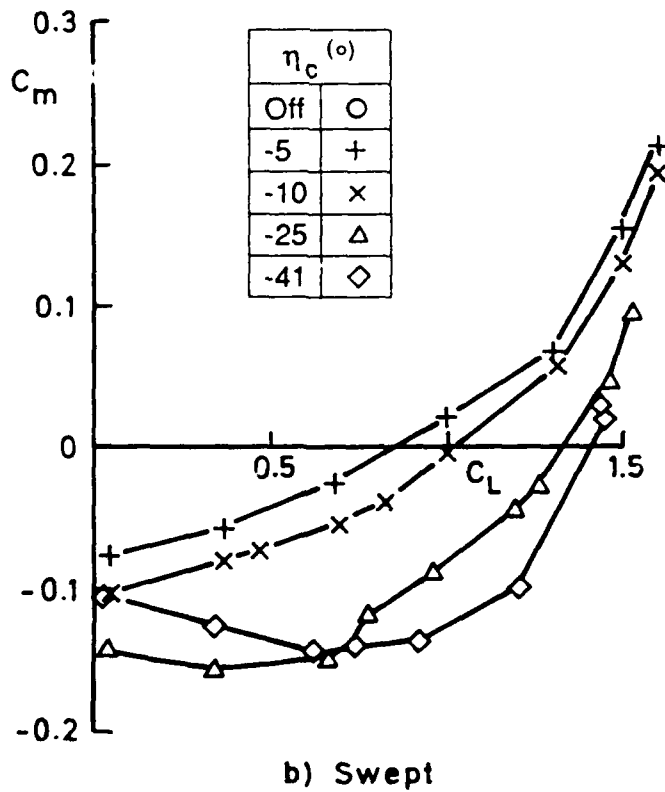
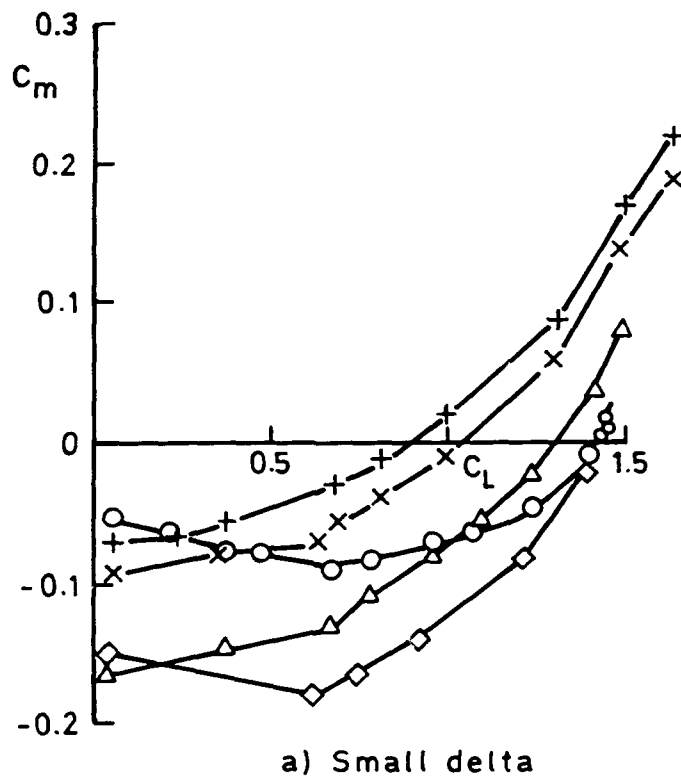
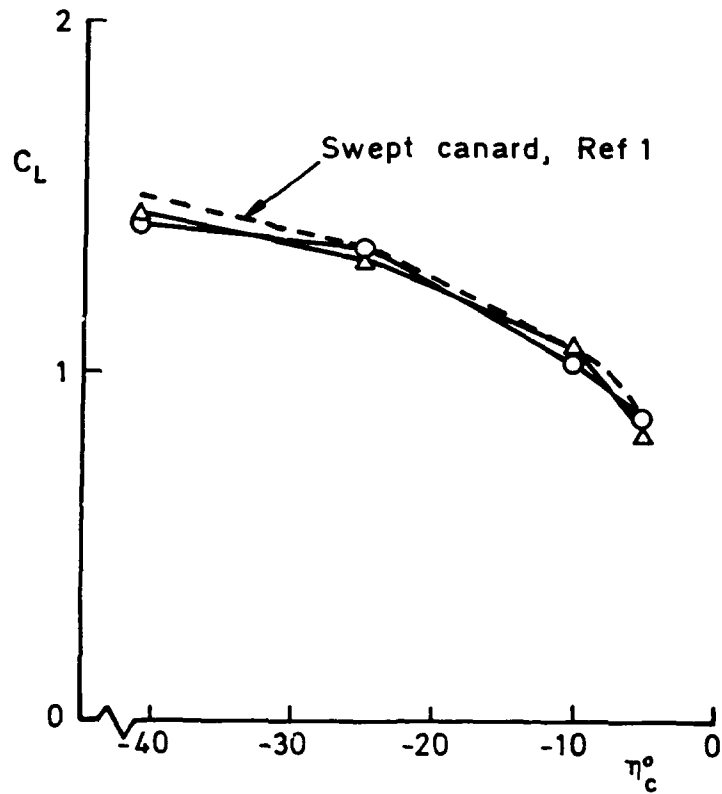
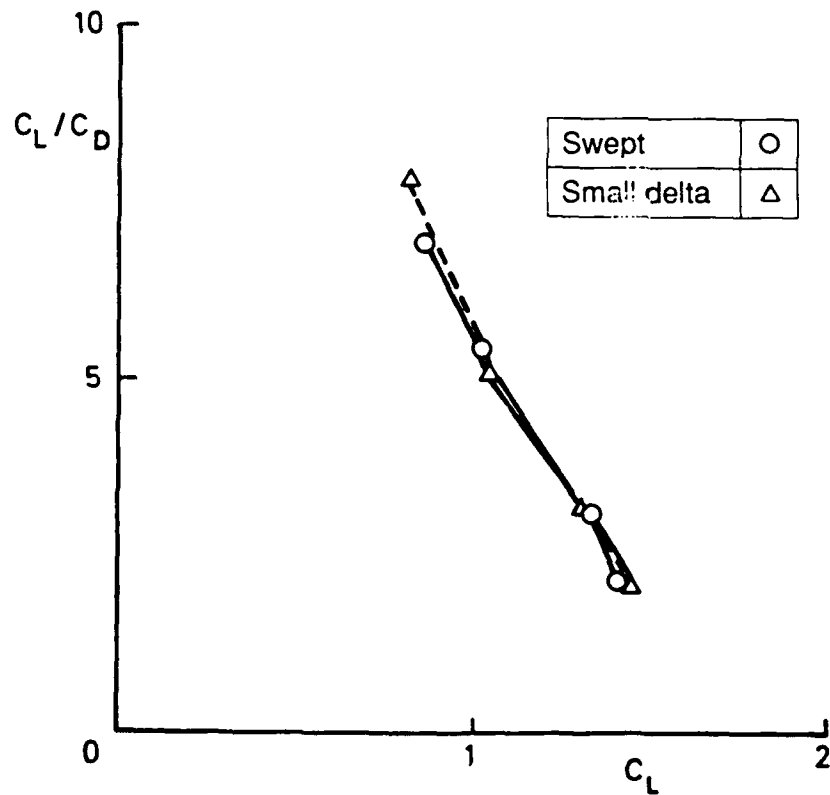


Fig 6 Effect of canards on control power

Fig 7



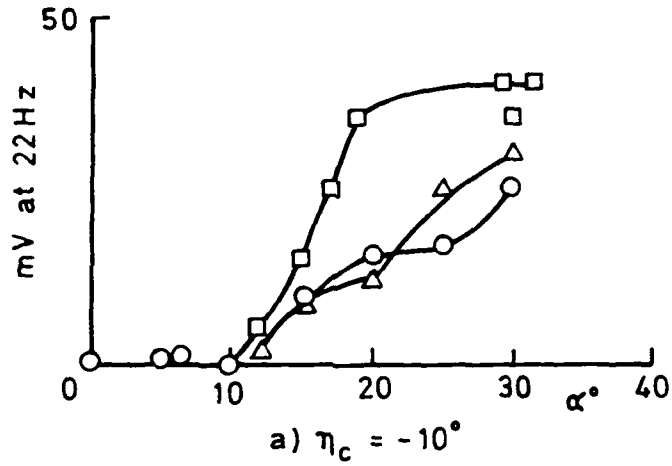
a) Trimmed C_L v canard setting



b) Lift/drag ratio v trimmed C_L

Fig 7 Effect of canards on drag

Fig 8



Canard	□
Small delta	△
Swept	○
Off	○

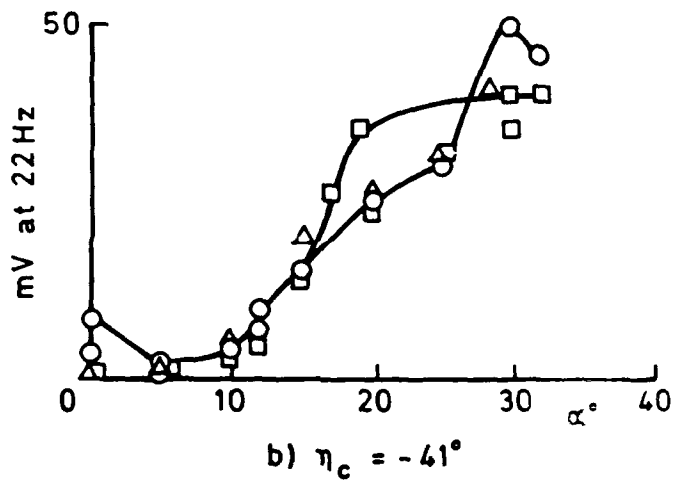
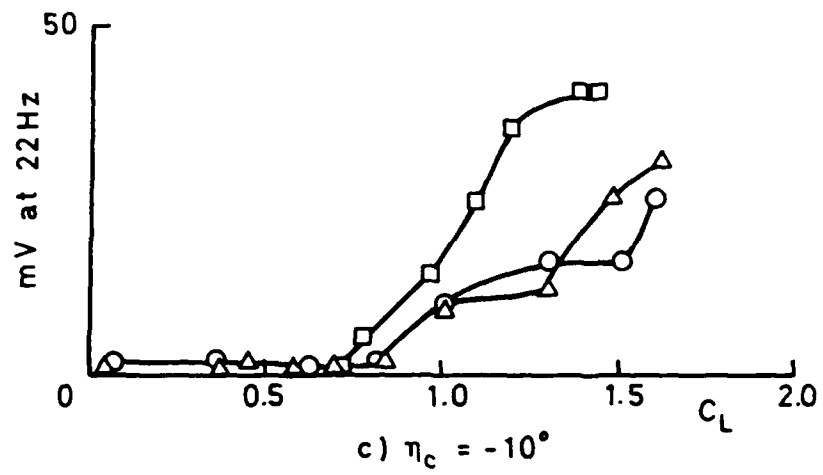


Fig 8 Effect of canards on wing buffeting



Canard	
Small delta	△
Swept	○
Off	□

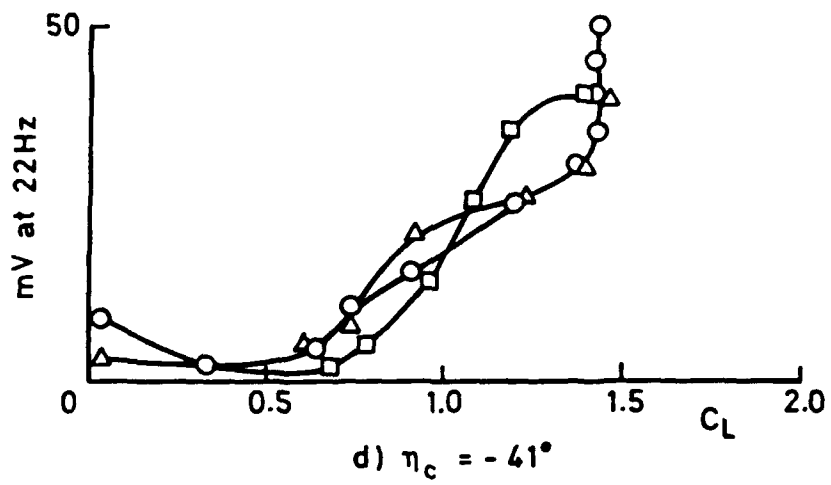
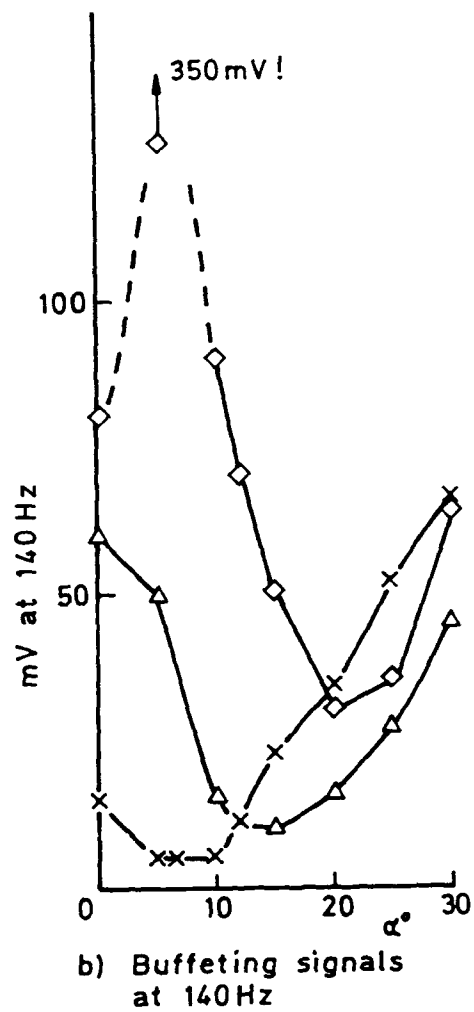
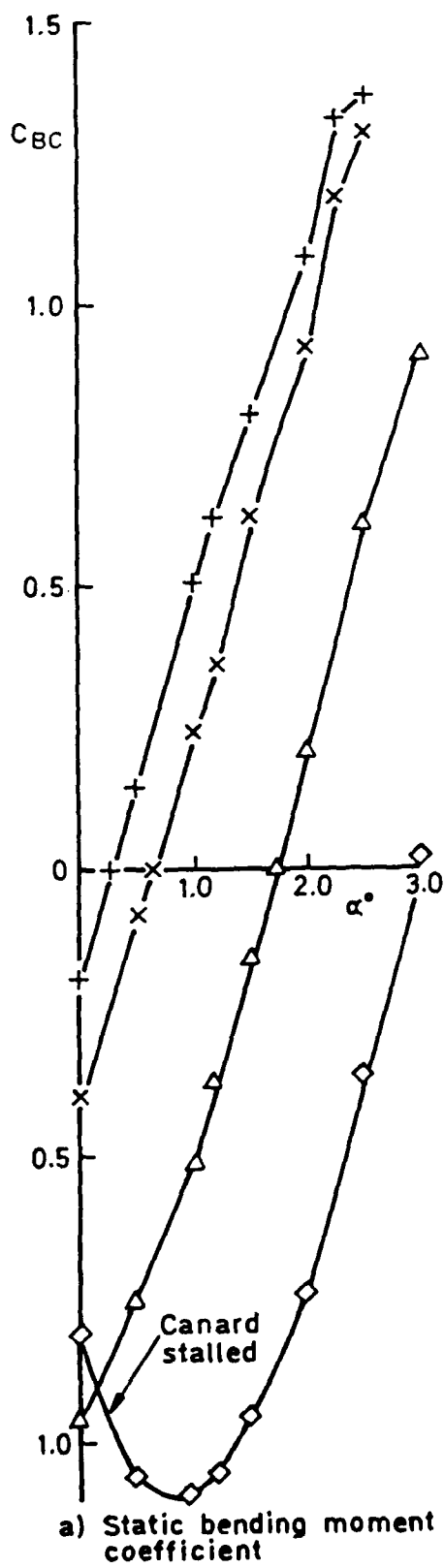


Fig 8 (concluded)

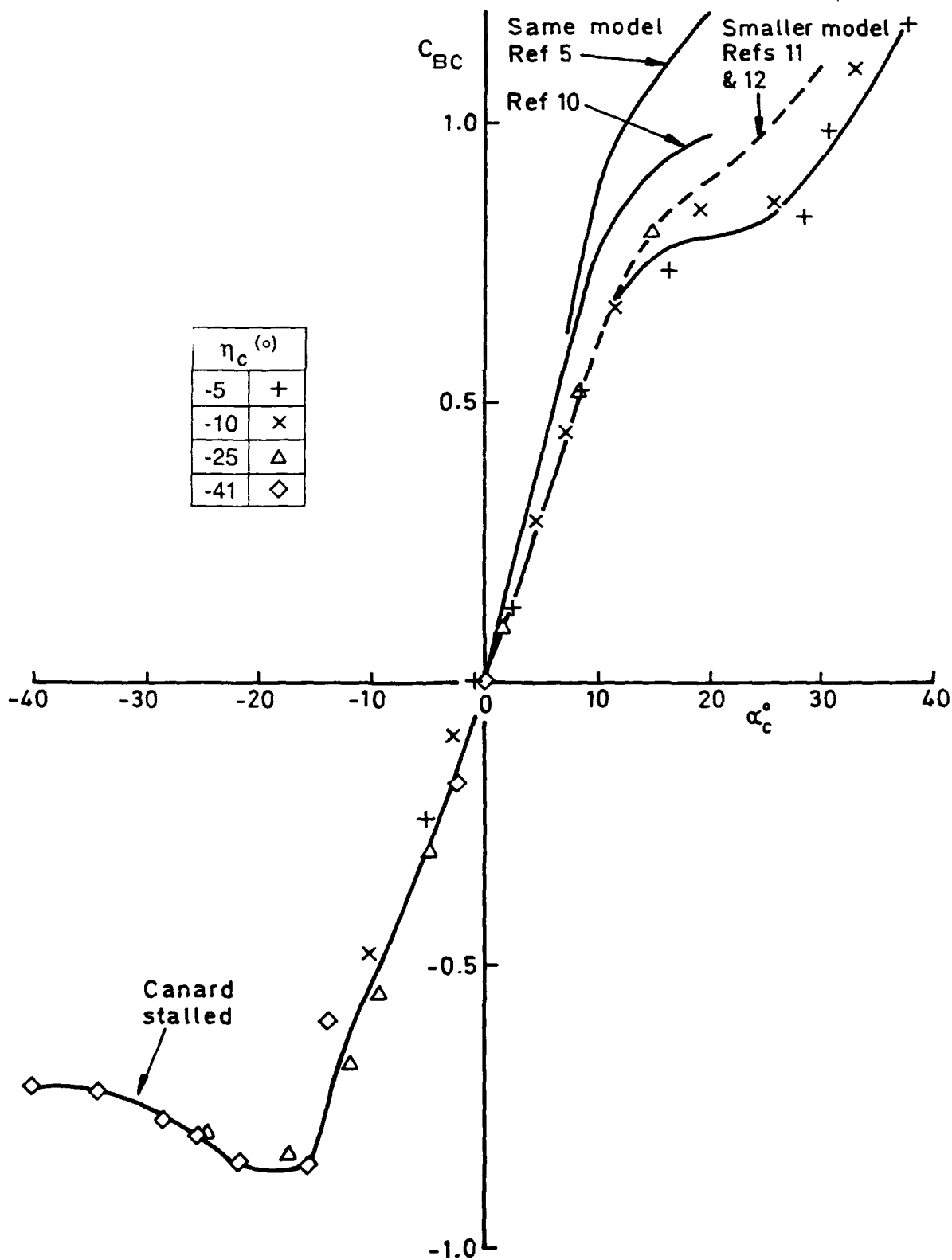
Fig 9



$\eta_c (^{\circ})$	
-5	+
-10	x
-25	Δ
-41	\diamond

Fig 9 Small delta canard - forces and buffeting as a function of angle of incidence

Fig 10



a) Static bending moment coefficient

Fig 10 Swept canard - forces and buffeting as a function of canard effective incidence

Fig 10 (conc)

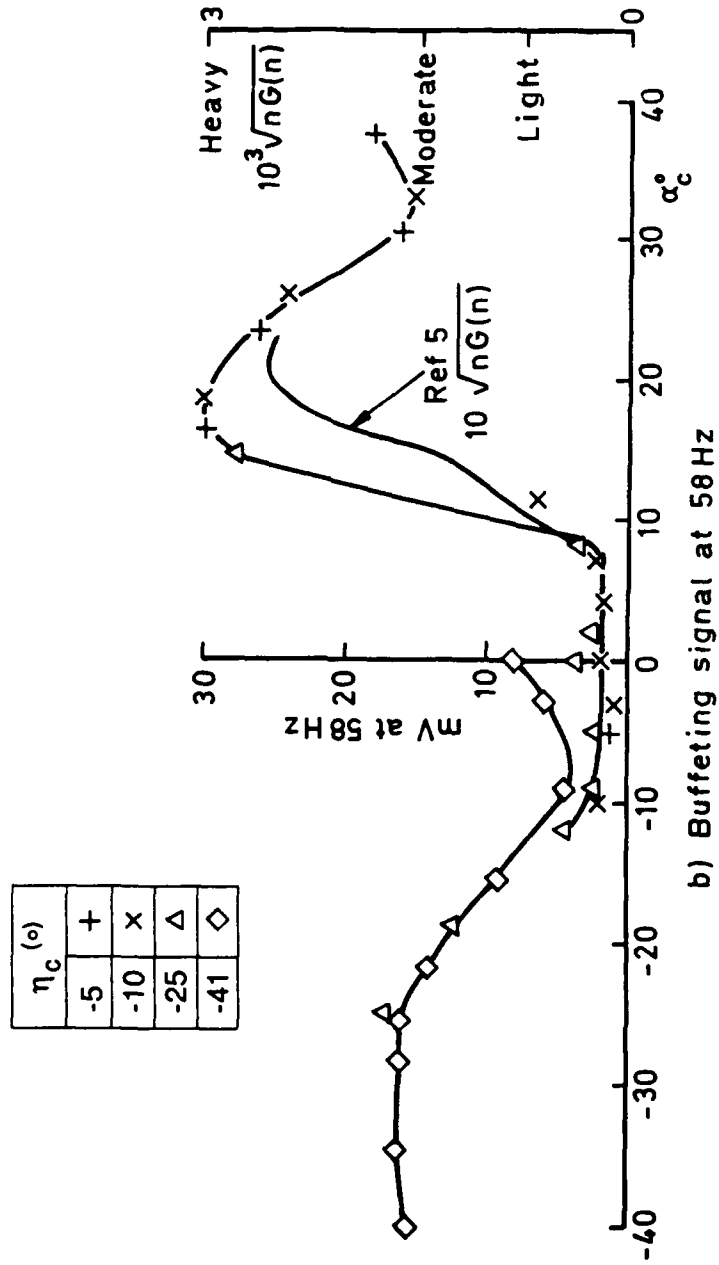


Fig 10 (concluded)

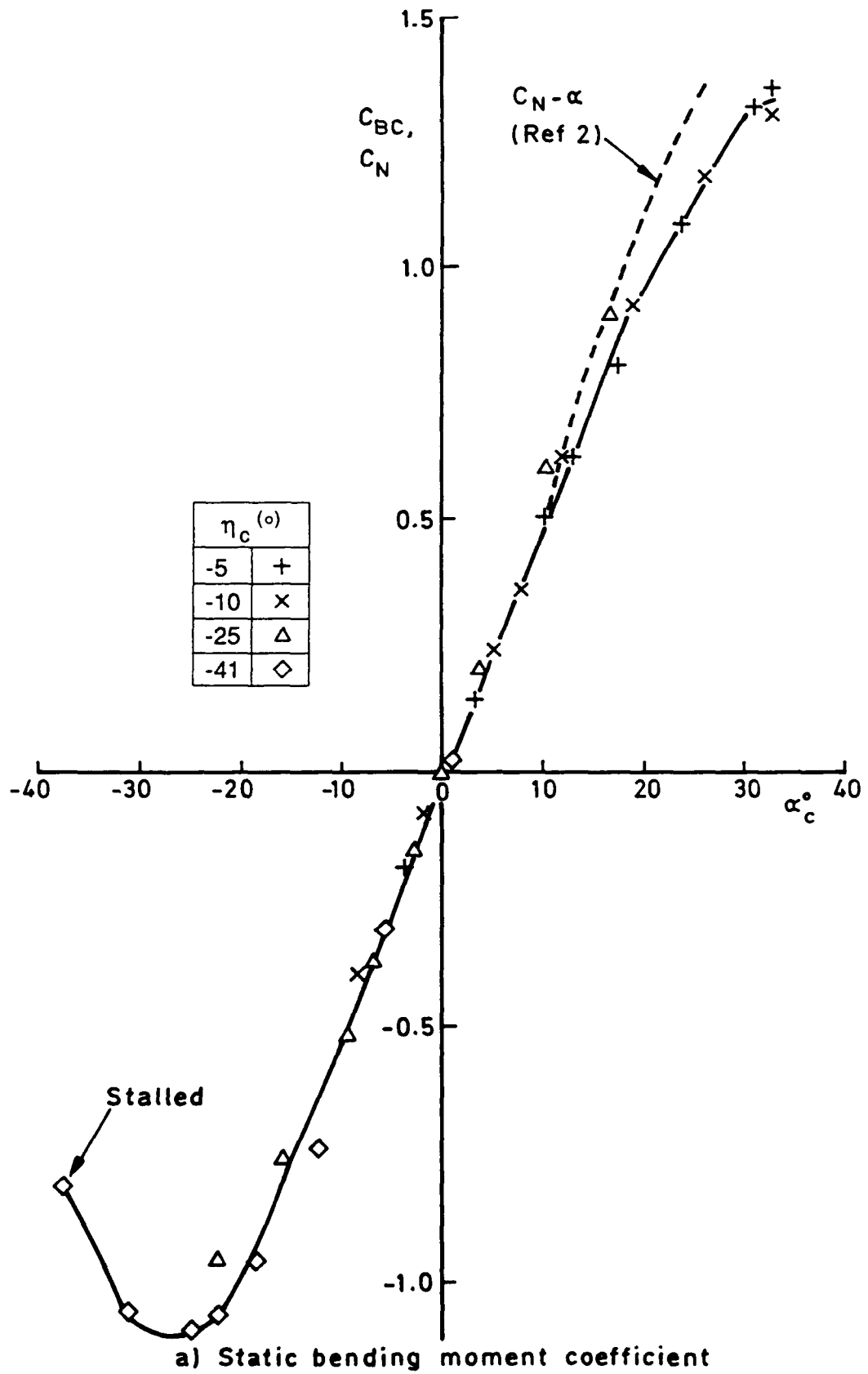


Fig 11 Small delta canard-forces and buffeting as a function of canard effective incidence

Fig11 (cont)

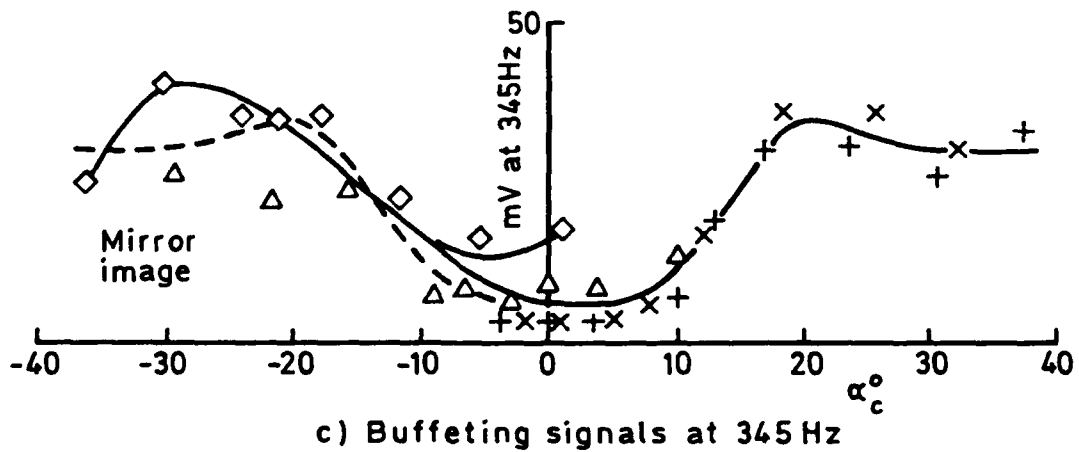
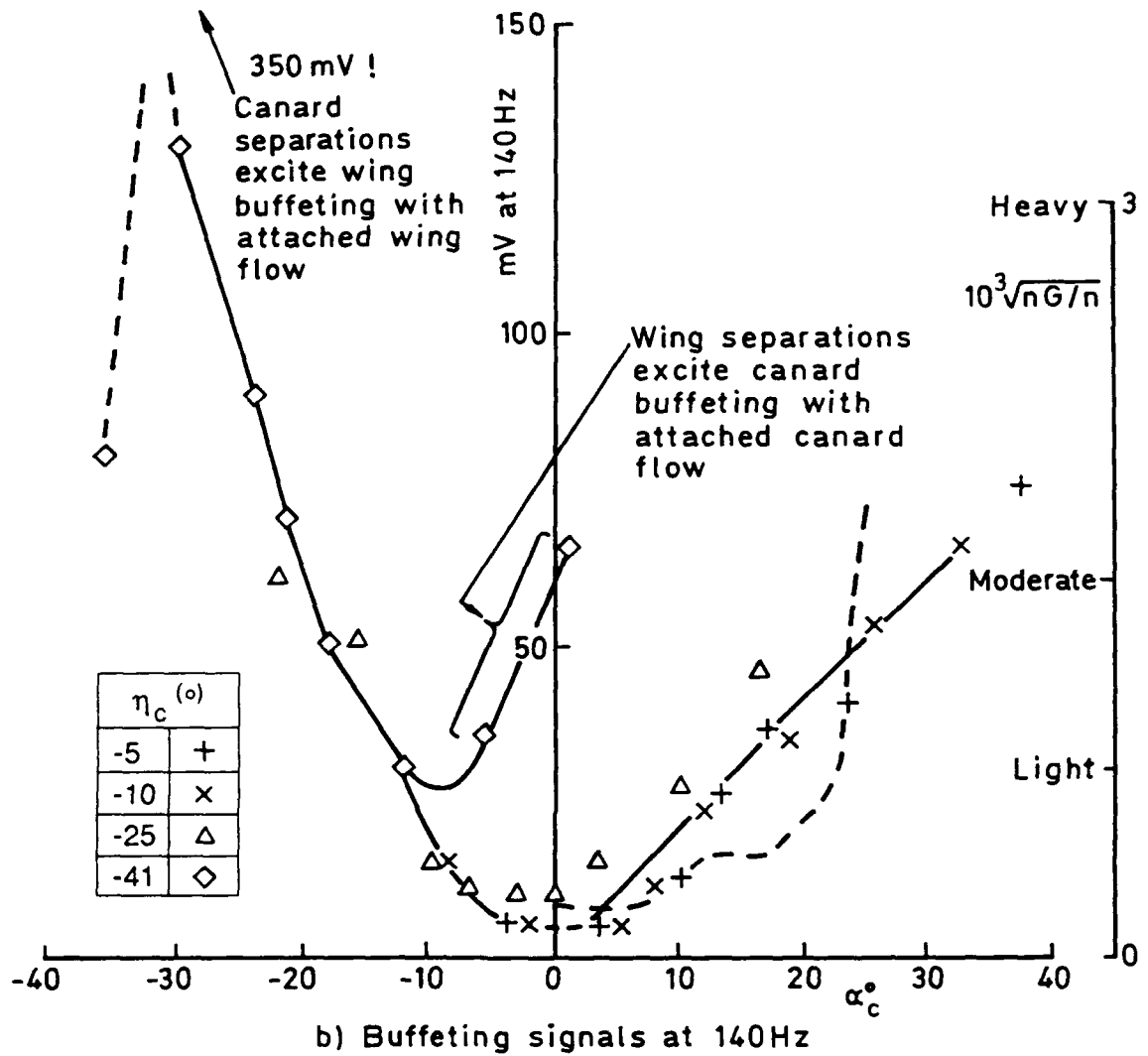
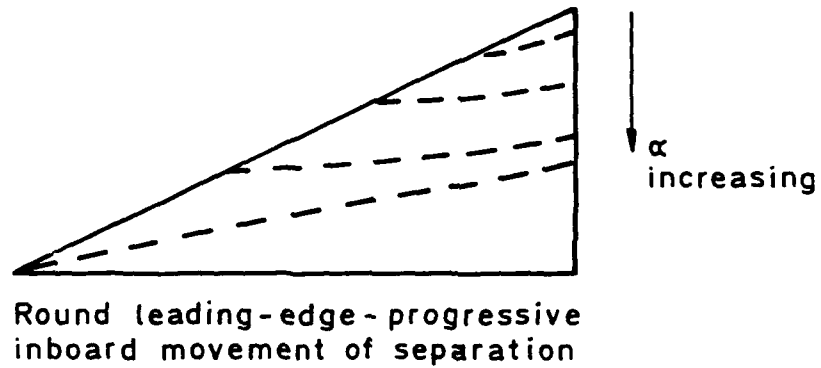
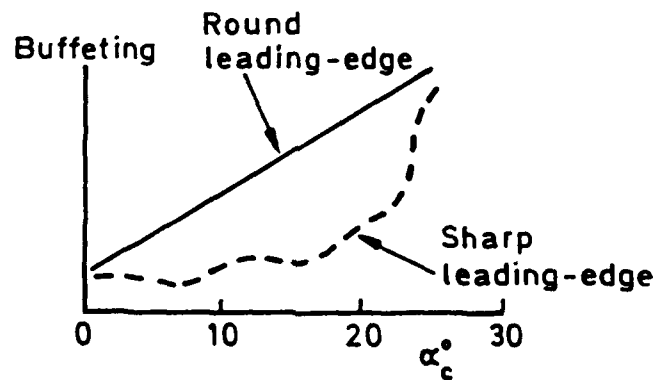
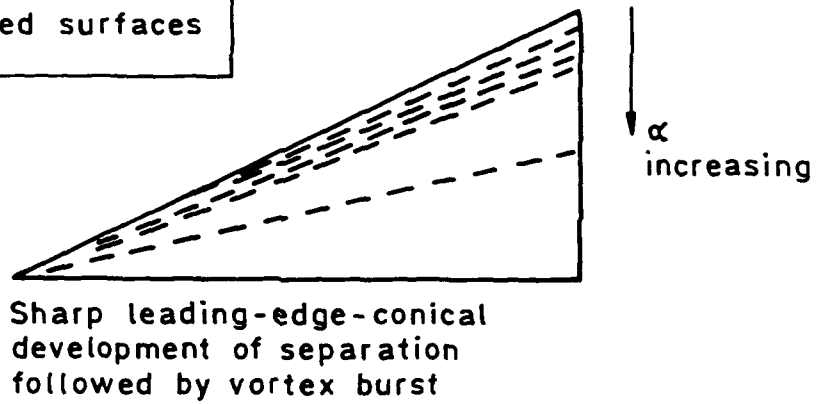


Fig 11 (continued)



Schematic only
Isolated surfaces



d) Effect of leading-edge shape on separation development and buffeting

Fig 12

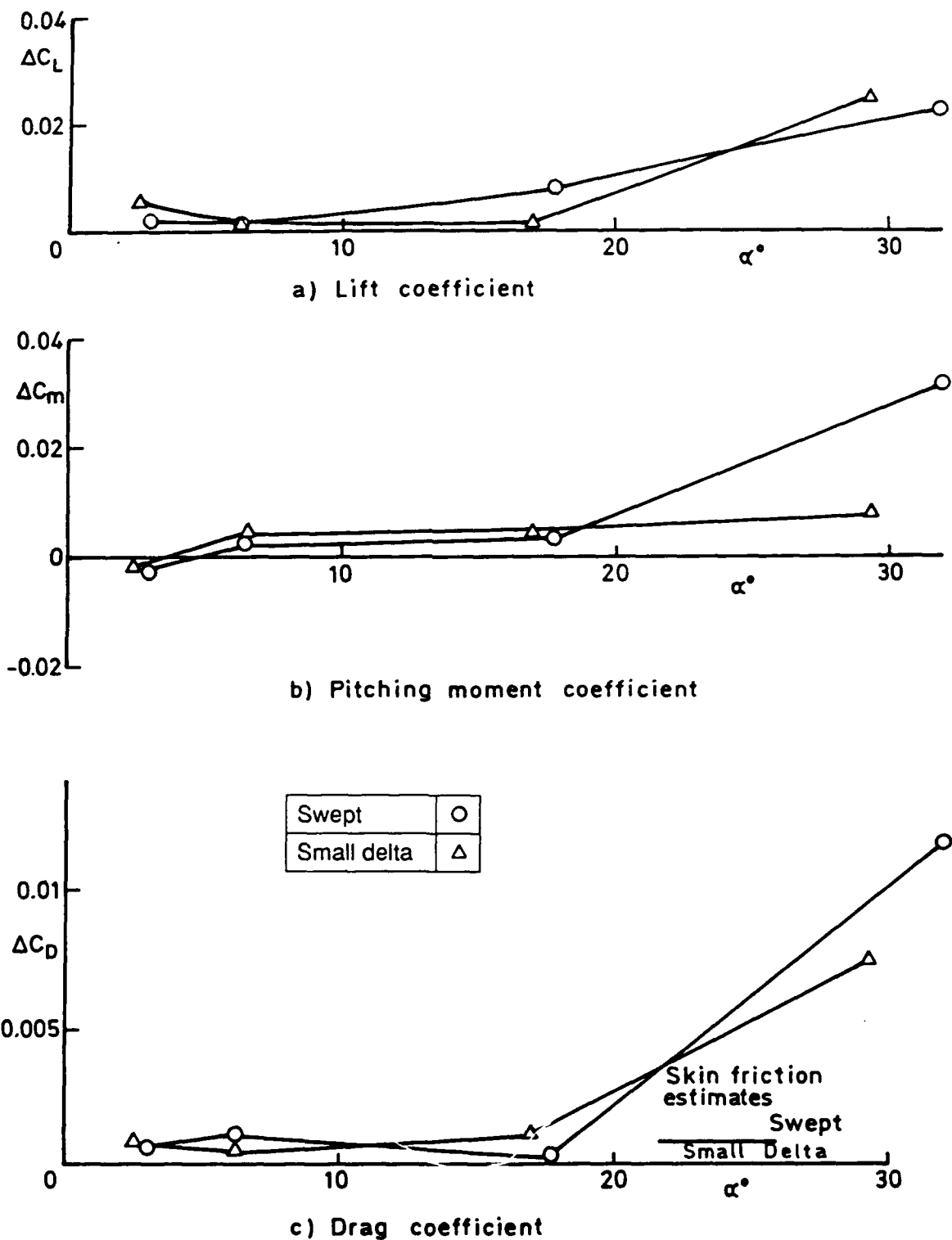


Fig 12 Force and moment increments due to canards for $\alpha_c = 0^\circ$ v angle of incidence

REPORT DOCUMENTATION PAGE

Report number and classification to this page

UNLIMITED

This report contains information only on unclassified information. If it is necessary to enter classified information, the box should be marked with the appropriate classification, e.g. Restricted, Confidential or Secret.

1. Report Number (Number by DRA)		2. Originator's Reference DRA TM A&P 23	3. Agency Reference N/A	4. Report Security Classification/Marking UNLIMITED		
5. Date for Originator 10/2000		6. Originator (Corporate Author) Name and Location DRA Bedford, Bedfordshire MK41 6AE				
7. Sponsoring Agency's Code 107508XX		6a. Sponsoring Agency (Contract Authority) Name and Location DD028, MOD Main Building				
7. Title Comparison between swept and delta canards on a model of a combat aircraft						
7a. (For Translations) Title in Foreign Language						
7b. (For Conference Papers) Title, Place and Date of Conference						
8. Author 1, Surname, Initials Milbey, D.G.	9a. Author 2 Pyne, C.R.	9b. Authors 3,4 ...		10. Date February 1993	Pages 31	Refs 12
11. Contract Number N/A	12. Period N/A	13. Project		14. Other Reference Nos.		
15. Distribution statement (a) Controlled by - Manager Aerodynamics/Propulsion Department (b) Special limitations (if any) - If it is intended that a copy of this document shall be released overseas refer to DRA Leaflet No. 3 to Supplement 6 of MOD Manual 4						
16. Descriptors (Keywords) (Descriptors marked * are selected from TEST) Unsteady aerodynamics. Canard surfaces. Canard/Delta configuration. Buffeting.						
17. Abstract <p>The aerodynamic characteristics of a low speed half model of a typical combat aircraft configuration fitted with a 55° delta canard planform are compared with those for the same model fitted with 44.3° swept canard. Both canards had an RAE 104 aerofoil section. The tests were made in the DRA 13 ft x 9 ft Wind Tunnel on a large model of the DRA High Incidence Research Model (HIRM 1), modified to represent the Experimental Aircraft (EAP) configuration.</p> <p>For a 15% smaller platform area, the delta canard gives higher lift and comparable pitching moments for trimming. For canard and wing buffeting the differences are small.</p> <p>Overall, these low speed measurements suggest that delta canards with round leading edges have significant advantages over swept canards for future combat aircraft.</p>						

ES910/1

Reproduced From
Best Available Copy

**END
FILMED**

DATE:

10-93

DTIC